

Heats of Dilution of Some Aqueous Rare Earth Electrolyte Solutions at 25 °C. 2. Rare Earth Nitrates

Frank H. Spedding,* John L. Derer, Michael A. Mohs, and Joseph A. Rard

Ames Laboratory-ERDA and Department of Chemistry, Iowa State University, Ames, Iowa 50011

The heats of dilution of the aqueous trinitrates of La, Pr, Nd, Sm, Gd, Tb, Dy, Ho, Er, Tm, Yb, and Lu have been measured from dilute solution to saturation at 25 °C. The integral heats of solution of $\text{La}(\text{NO}_3)_3 \cdot 6\text{H}_2\text{O}$, $\text{Nd}(\text{NO}_3)_3 \cdot 6\text{H}_2\text{O}$, $\text{Gd}(\text{NO}_3)_3 \cdot 6\text{H}_2\text{O}$, $\text{Ho}(\text{NO}_3)_3 \cdot 6\text{H}_2\text{O}$, $\text{Er}(\text{NO}_3)_3 \cdot 6\text{H}_2\text{O}$, and $\text{Lu}(\text{NO}_3)_3 \cdot 5\text{H}_2\text{O}$ in water have also been determined. The heat of dilution data were fitted directly to semiempirical polynomials and these polynomials were used to calculate apparent and partial molal heat quantities. The results are compared to available thermodynamic and transport data for the rare earth nitrates.

The electrical conductances (12) and partial molal volumes (18) of rare earth nitrate solutions exhibit behavior considerably different from that found for the corresponding rare earth chloride and perchlorate solutions. The rare earth chloride and perchlorate solutions are believed to contain only outer sphere complexes; consequently, their thermodynamic and transport properties seem to be directly correlated with changes in rare earth ion hydration across the rare earth series. For the rare earth nitrates, appreciable amounts of inner sphere complexes are formed (1, 2, 6) in addition to outer sphere complexes, and their presence would be expected to greatly affect hydration trends. Furthermore, rare earth nitrate thermodynamic (18) and transport (12) properties seem to be correlated with the trend in the stability constants (2, 11).

The heats of dilution of rare earth nitrate solutions should depend strongly on changes in the amounts of inner and outer sphere complexes with concentration and the variation of their heats of dissociation with rare earth. Changes in ionic hydration and electrical work with concentration also affect these heats. By comparing the nitrate heat data to the corresponding data for rare earth perchlorate solutions (16), which presumably contain no inner sphere complexes, it is possible to make a qualitative assessment of the importance of nitrate complexes on the thermodynamic behavior of these solutions. In addition, heat of dilution data are valuable since they can be used to calculate the temperature derivatives of the activity coefficients (13).

Experimental Section

An adiabatic differential calorimeter was used that is similar to Gucker et al. (7). This calorimeter has been described in detail elsewhere (4, 8). The solution samples were contained in thin-walled annealed Pyrex bulbs. One 10–20-ml sample bulb was used for dilute solutions, and two 4–10-ml sample bulbs were used for each run at higher concentrations. Dilutions were made into conductivity water (specific conductivity less than 1×10^{-6} ohm $^{-1}$ cm $^{-1}$) and the total weight of each solution sample plus conductivity water was fixed at about 900 g. The accuracy of the calorimeter measurements was checked by heat of neutralization experiments. After extrapolation of these data to infinite dilution, the negative of the heat of ionization of water was obtained (given in the perchlorate heat paper (16)) and was found to be in excellent agreement with other experimental values. All experimental heats were corrected for the heat of opening of the bulbs and for the evaporation of water into the volume

originally occupied by air in the sample bulbs, using experimental osmotic coefficient data (13). All of these heats were measured at 25.00 ± 0.02 °C and 1 cal = 4.1840 absolute J was used in the calculations.

Stock solutions of the stoichiometric rare earth nitrates were prepared by the method of Spedding et al. (17) from ion-exchange purified rare earth oxides. The purity of these rare earth oxides was 99.85% or better by weight, with adjacent rare earths, calcium, iron, and silicon being the principal impurities. The amount of impurities present was less than the quantitative detection limit in most cases, so 0.15% impurities is an upper limit.

The stock and saturated solutions were analyzed by EDTA and gravimetric sulfate methods, and the resulting concentrations are reliable to $\pm 0.1\%$ or better in terms of the molality. The nitrate samples were decomposed by heating with hydrochloric acid before the sulfate precipitations were performed, to avoid nitrate ion coprecipitation. The dilutions were prepared by weight from the stock solutions. Conductivity water was used in all solution preparations and all weights were converted to vacuum. Hydrated crystals were grown from saturated solutions at 25 °C and the hydrate compositions were determined by EDTA analyses. After drying, the hydrates were found to be within ± 0.016 water molecules of the indicated hydrate.

Calculations and Errors

Consider a sample of rare earth nitrate solution at a molality m_1 , containing n' moles of salt, being diluted to a molality m_2 , and giving off q' calories of heat. Then,

$$q' = n'[\phi_L(m_2) - \phi_L(m_1)] \quad (1)$$

where ϕ_L is the relative apparent molal heat content of the solution at the molality in parentheses. If a second sample, containing n'' moles of salt, is added to the previous solution, and q'' calories of heat are given off, then,

$$q'' = (n' + n'')\phi_L(m_3) - n''\phi_L(m_1) - n'\phi_L(m_2) \quad (2)$$

where m_3 is the molality of the solution with both samples added. It should be noted that heat of dilution experiments give only enthalpy differences and not absolute values.

If the experimental heats are converted to per mole of salt, the integral heats of dilution

$$\Delta H_{1,2} = q'/n' \quad (3)$$

and

$$\Delta H_{1,3} = (q' + q'')/(n' + n'') \quad (4)$$

are obtained. In the dilution experiments, the initial molality ranged from about 0.01–0.05 m to saturation and the samples were diluted to a few millimolar in concentration. If a second sample is diluted into the solution resulting from the first sample,

$$\Delta H_{3,2} = \Delta H_{1,2} - \Delta H_{1,3} \quad (5)$$

These heat differences can be used to give information about the heats of dilution for very dilute solutions, since this heat difference corresponds to a dilution process from m_3 to m_2 .

Table I. Heats of Dilution of Some Aqueous Rare Earth Nitrate Solutions at 25 °C

m_i	$10^4 m_f$	Exptl					Exptl			
		$-\Delta H_{i,f}$, cal/mol	—calcd		σ , cal/mol	m_i	$10^4 m_f$	$-\Delta H_{i,f}$, cal/mol	—calcd	
			ΔH , cal/mol	σ , cal/mol					ΔH , cal/mol	σ , cal/mol
Lanthanum Nitrate										
4.608	30.504	1524.5	1.2	2.8	0.006 637	30.515	116.8	-3.6	3.8	
	66.374* ^a	1409.6	2.4	3.5	0.005 727	28.430	114.9	-1.2	3.8	
	30.515	1528.5	-2.8	2.8	0.005 747	28.313	96.7	2.6	3.2	
4.456	66.178*	1411.7	0.8	3.5	0.009 815	48.595	102.6	-2.2	3.2	
	28.313	1460.7	-2.6	2.4	0.009 718	48.136	113.6	1.4	4.2	
	57.472*	1358.1	-0.4	2.9	0.005 127	25.341	97.7	-1.1	2.1	
4.000	28.430	1455.4	2.1	2.4	0.005 107	25.422	98.3	-2.7	2.1	
	57.275*	1358.7	-0.5	2.9	0.002 870	14.334	82.5	-3.6	2.3	
	48.136	1164.2	1.5	3.1	0.002 884	14.334	83.9	-4.4	2.3	
3.606	97.180*	1050.5	0.6	3.8	0.003 904	19.705	89.4	-3.1	2.0	
	48.595	1166.9	-2.6	3.1	0.003 919	19.651	88.7	-1.5	2.0	
	98.149*	1053.3	-4.0	3.8	0.004 747	23.951	93.5	-1.6	2.1	
3.239	25.422	1074.4	1.4	1.6	0.004 736	24.020	93.3	-2.1	2.1	
	51.065*	976.1	4.1	1.9						
	25.341	1075.4	0.8	1.6						
Praseodymium Nitrate										
2.893	51.266*	977.7	1.9	1.9	4.990	11.672	—	—	—	
	14.334	988.3	-2.0	1.7		23.792*	2008.2	-8.6	1.7	
	28.837*	904.4	2.4	2.1		11.447	2068.9	5.4	1.6	
2.557	14.334	992.6	-6.3	1.7		25.521*	1986.6	4.8	2.3	
	28.697*	910.1	-2.7	2.1	4.833	15.897	1940.1	1.9	1.9	
	19.651	820.3	0.9	1.5		32.435*	1862.5	-1.6	2.6	
2.092	39.188*	731.6	2.4	1.8	4.465	29.026	1657.7	-4.7	2.8	
	19.705	825.0	-4.1	1.5		56.874*	1563.2	-1.4	3.6	
	39.038*	735.6	-1.0	1.8		30.348	1651.8	-4.3	2.8	
1.960	24.020	684.9	1.9	1.5		57.095*	1563.6	-2.4	3.6	
	47.362*	591.6	4.0	1.9	4.002	29.619	1391.5	1.8	2.4	
	23.951	687.3	-0.1	1.5		60.850*	1293.2	1.3	3.3	
1.694	47.472*	593.8	1.5	1.9		29.148	1395.0	0.2	2.4	
	29.322	543.0	3.6	1.3		61.532*	1292.1	0.7	3.4	
	29.268	546.0	0.8	1.3	3.618	29.500	1186.6	7.8	2.5	
1.341	34.293	523.0	2.9	1.3		27.608	1191.4	11.1	1.9	
	28.143	532.0	-2.8	1.4		54.937*	1107.1	3.2	2.5	
	27.552	534.0	-2.1	1.4	3.444	31.994	1100.2	-2.3	2.0	
0.810 1	35.082	503.0	-2.7	1.4		64.678*	1002.1	-2.6	2.7	
	25.412	514.0	-1.0	1.9		31.273	1108.1	-7.3	1.9	
	25.492	515.0	-2.4	1.9		59.614*	1015.8	-4.0	2.4	
0.639 7	26.225	512.0	-3.7	2.2	2.978	27.082	905.8	-2.6	1.5	
	20.367	541.0	-2.7	2.2		55.006*	810.1	-1.6	1.9	
	20.385	542.0	-3.8	2.2		27.657	—	—	—	
0.489 1	30.437	501.0	0.0	1.5		55.401*	809.0	-1.6	1.5	
	30.559	499.0	1.5	1.5	2.564	36.139	701.1	0.6	1.4	
	51.840	454.0	2.7	1.7		72.379*	599.1	2.5	1.8	
0.359 8	51.768	456.0	0.9	1.7		36.861	699.6	-0.5	1.5	
	59.970	471.0	3.3	2.0		72.703*	599.6	1.3	1.8	
	60.187	473.0	0.7	2.0	2.200	43.186	559.7	1.2	1.3	
0.249 8	56.250	526.0	1.2	2.1		85.265*	461.9	-3.2	1.7	
	56.490	525.0	1.5	2.1		42.909	560.8	1.0	1.3	
	22.184	697.0	-4.9	1.8		85.396*	457.2	1.3	1.7	
0.159 9	52.751	575.0	0.2	1.8	1.922	56.614	456.7	-0.7	1.9	
	52.432	575.0	1.1	1.8		57.553	451.3	2.3	1.9	
	32.718	666.0	3.4	1.6	1.684	58.723	409.3	3.6	1.8	
0.098 97	32.149	669.0	2.7	1.6		56.925	418.9	-1.4	1.7	
	26.998	705.0	-5.0	1.4		56.975	419.0	-1.6	1.7	
	27.374	707.0	-8.7	1.4	1.448	52.398	411.5	0.0	1.6	
0.017 02	26.389	676.0	2.5	1.3		51.195	415.3	-0.4	1.6	
	26.729	676.0	0.9	1.3	1.226	50.327	418.6	-0.2	1.6	
	17.447	725.0	1.4	1.3		50.606	421.6	-4.0	1.6	
0.009 027	11.016	715.0	0.9	2.9	1.106	46.917	435.9	0.4	1.5	
	11.350	708.0	5.2	2.9		45.570	440.2	0.2	1.5	
	15.257	673.0	11.5	2.9	0.917 4	38.480	483.6	2.2	1.4	
0.017 02	11.243	705.0	9.1	2.9		38.571	485.5	0.0	1.4	
	1.1946	540.0	-14.8	10.0	0.643 0	27.532	580.7	-3.2	1.3	
	1.2837	554.0	-31.3	10.0		27.511	578.4	-0.8	1.4	
0.009 027	0.9860	417.0	-1.7	10.0	0.500 6	26.814	608.1	1.2	1.3	
	0.9807	442.0	-26.6	10.0		28.060	600.3	3.6	1.3	

Table I. Continued

m_i	$10^4 m_f$	Exptl					Exptl		
		$-\Delta H_{i,f}$, cal/mol	ΔH , cal/mol	σ , cal/mol	m_i	$10^4 m_f$	$-\Delta H_{i,f}$, cal/mol	ΔH , cal/mol	σ , cal/mol
0.358 2	19.314	671.1	-0.9	1.9	1.755	25.908	488.0	-0.3	2.1
	38.098*	590.1	-1.6	3.2		52.201*	398.7	0.9	2.6
	19.496	—	—	—		25.806	492.1	-4.0	2.1
	38.608*	589.4	-2.7	2.6		53.949*	395.9	-0.9	2.6
0.253 4	16.837	687.3	2.8	2.1	1.491	44.769	384.0	1.7	1.5
	33.097*	611.5	0.7	3.4		30.239	433.0	2.1	1.5
0.169 3	21.581	654.4	-6.9	1.7	1.250	48.177	367.0	-0.7	1.3
	20.129	654.5	0.7	1.9		49.182	363.0	0.5	1.3
0.099 97	14.846	632.0	4.6	2.7	1.032	53.568	362.0	-0.7	1.6
	14.910	633.1	3.1	2.7		63.187	336.0	2.1	1.6
	8.2285	590.2	1.6	3.6		71.470	319.0	1.3	1.6
0.051 27	8.3510	586.5	4.1	3.6	0.834 2	66.945	352.0	0.7	1.7
	3.1114	501.3	-17.9	4.3	0.659 5	47.513	430.0	2.3	1.7
0.019 27	3.2329	482.5	-1.2	4.3		62.189	361.0	0.1	1.5
	11.447	82.3	0.6	2.5		44.836	439.0	-1.2	1.5
0.003 243	15.897	77.6	3.5	2.8	0.490 8	46.335	470.0	-3.6	1.5
	29.026	94.5	-3.3	4.0		49.745	462.0	-5.2	1.5
0.005 710	30.348	88.3	-2.0	3.9	0.369 7	31.450	538.0	-0.6	1.4
	29.619	98.3	0.5	3.6		27.009	554.0	1.3	1.4
0.006 085	29.148	102.8	-0.4	3.7	0.253 3	22.829	584.0	1.6	1.9
	27.608	84.3	7.9	2.8		22.203	585.0	3.7	1.9
0.006 468	31.994	98.1	0.3	2.9	0.163 9	16.322	607.0	3.0	2.6
	31.273	92.2	-3.3	2.7		16.040	608.0	3.7	2.6
0.005 961	27.082	95.7	-1.0	2.1	0.102 4	8.5849	628.0	3.4	3.6
	36.139	102.0	-1.9	2.0		7.2307	638.0	6.4	3.6
0.007 270	36.861	100.1	-1.9	2.0	0.040 35	3.3526	584.0	-11.0	10.0
	43.186	97.7	4.4	1.9	0.010 22	0.8178	435.0	-24.8	10.0
0.008 527	42.909	103.6	-0.3	1.9	0.003 823 ^b	17.247	88.5	1.9	2.8
	19.314	81.0	0.8	3.4	0.003 782	15.484	99.5	0.1	2.8
0.003 810	16.837	75.8	2.0	3.6	0.004 216	20.603	88.9	-4.2	2.7
					0.004 529	23.542	81.7	-2.0	2.7
Neodymium Nitrate									
4.582	15.484	1844.1	2.3	2.0	0.006 282	32.890	87.2	-1.3	2.9
	37.822*	1744.6	2.2	2.5	0.005 977	30.758	87.7	-0.8	2.9
	17.247	1834.4	1.4	2.0	0.006 156	33.086	84.5	-2.2	2.5
	38.229*	1745.9	-0.5	2.5	0.005 721	28.270	93.1	-2.4	2.5
4.144	23.542	1543.3	-3.6	2.0	0.006 376	33.733	81.5	3.4	2.2
	45.293*	1461.6	-1.5	2.4	0.003 728	20.476	74.2	-4.6	2.2
	20.603	1559.8	-5.6	2.0	0.003 629	17.834	84.2	-3.7	2.2
	42.159*	1470.9	-1.4	2.4	0.003 643	18.071	82.9	-3.3	2.8
3.618	30.758	1209.7	1.5	2.1	0.003 575	16.622	88.8	-3.2	2.8
	59.768*	1122.0	2.3	2.6	0.005 875	31.014	81.7	1.8	2.3
	32.890	1203.7	-0.6	2.1	0.005 806	29.681	88.7	-1.6	2.3
	62.821*	1116.5	0.7	2.6	0.005 395	25.806	96.2	-3.1	2.9
3.394	28.270	1103.1	-1.5	1.8	0.005 220	25.908	89.3	-1.2	2.9
	57.214*	1010.0	0.9	2.3					
3.036	33.086	1083.8	-1.0	1.8					
	61.560*	999.3	1.3	2.3	4.284				
2.662	33.954	898.3	2.0	1.6		15.802	1792.0	1.6	1.7
	63.123*	815.0	2.6	2.0		29.737*	1731.9	0.2	2.2
2.368	33.733	890.8	10.3	1.6		14.409	1802.8	-1.2	1.7
	63.760*	809.3	6.9	2.0	3.827	31.842*	1720.3	4.5	2.5
	17.834	811.4	-6.3	1.6		18.780	1459.8	-6.9	1.7
	36.289*	727.2	-2.6	2.0		37.463*	1388.4	-6.2	2.2
2.033	20.476	796.4	-5.6	1.6		20.313	1442.8	2.7	1.7
	37.283*	722.2	-1.0	2.0	3.461	38.787*	1375.2	3.1	2.2
	16.622	701.9	-2.7	2.0		24.635	1180.9	-0.6	1.7
	35.748*	613.1	0.5	2.5		48.859*	1108.0	-2.5	2.3
2.033	18.071	699.1	-8.2	2.0		25.643	1177.5	-1.3	1.8
	36.433*	616.2	-4.9	2.5	3.228	52.177*	1097.2	0.6	2.4
	29.681	533.7	-0.7	1.7		30.097	1006.4	5.2	1.8
	58.064*	445.0	0.9	2.1		59.452*	928.9	5.2	2.3
2.033	31.014	523.0	4.7	1.7		58.023*	935.6	1.4	2.3
	58.752*	441.3	2.9	2.1	2.778	31.633	742.8	1.8	1.4
						63.544*	664.8	-0.6	1.8
						31.542	743.2	1.7	1.4
						63.867*	662.9	0.7	1.8

Table I. Continued

<i>m_i</i>	10 ⁴ <i>m_f</i>	Exptl — calcd					Exptl — calcd			
		—Δ <i>H_{i,f}</i> , cal/mol	Δ <i>H</i> , cal/mol	σ, cal/mol	<i>m_i</i>	10 ⁴ <i>m_f</i>	—Δ <i>H_{i,f}</i> , cal/mol	Δ <i>H</i> , cal/mol	σ, cal/mol	
2.457	70.313	486.0	4.1	2.4	2.896	11.580	1293.4	4.6	1.1	
	70.052	491.9	—1.4	2.4		27.342*	1206.9	2.6	1.3	
	35.222	572.3	—1.1	1.1		13.757	1288.7	—6.4	1.1	
	70.083*	491.6	—1.1	1.7		27.217*	1213.6	—3.6	1.3	
	36.508	569.6	—2.3	1.1	2.566	19.351	—	—	—	
	72.004*	488.8	—1.7	1.7		44.556*	952.0	1.9	1.5	
	70.909	348.7	1.7	1.8		19.316	1058.5	—3.7	1.4	
2.125	71.201	348.1	1.8	1.8		43.745*	956.4	0.0	1.7	
	132.806	206.9	—0.7	2.0	2.254	21.178	884.6	4.9	1.1	
1.935	133.916	206.9	—1.8	2.0		43.217*	798.7	3.9	1.4	
	180.097	94.3	0.1	1.3		19.981	899.3	—3.5	1.1	
1.647	178.929	95.3	—0.1	1.3		45.064*	796.8	0.2	1.4	
	186.943	60.5	—4.0	2.3	1.967	30.592	731.6	0.6	1.2	
1.428	143.633	91.0	—0.5	1.9		59.413*	643.6	—0.3	1.5	
	65.631	188.3	2.1	2.1		28.026	746.6	—3.8	1.2	
	65.946	186.5	3.3	2.1		57.517*	649.1	—1.1	1.5	
1.124	126.406	97.1	—1.9	2.1	1.692	46.581	597.1	—0.9	1.5	
	126.771	95.7	—0.9	2.1		98.188*	486.0	—1.1	1.9	
0.978 1	99.803	133.6	0.8	1.9		49.787	584.5	2.5	1.5	
	101.536	132.1	0.1	1.9		100.701*	480.9	—0.1	1.9	
0.804 5	85.703	174.8	0.8	1.5	1.440	60.637	508.0	2.5	2.2	
	84.026	176.7	1.4	1.6		59.444	510.0	3.4	2.2	
0.653 2	48.414	277.6	—4.2	1.9	1.211	77.934	452.0	—1.4	2.4	
	57.000	252.1	1.9	1.7		64.417	480.0	—0.6	2.4	
0.440 2	58.020	252.0	—0.1	1.6	1.004	84.824	434.0	0.0	2.5	
	51.873	311.4	2.0	1.3		77.651	449.0	—1.3	2.5	
0.345 0	51.816	312.5	1.0	1.3	0.811 4	67.125	478.0	0.4	2.2	
	38.289	371.5	—2.0	1.7		63.409	487.0	—0.2	2.2	
0.265 5	37.021	375.0	—1.8	1.8	0.641 7	50.410	534.0	—0.5	2.1	
	28.582	418.4	—3.2	2.2		60.591	507.0	0.2	2.1	
0.149 5	28.817	417.2	—2.8	2.2		55.235	522.0	—1.4	2.1	
	17.875	463.2	0.9	2.9	0.498 0	43.983	561.0	3.6	1.9	
0.099 23	16.252	471.9	0.9	3.1		53.057	536.0	2.6	1.9	
	14.812	457.4	6.0	3.2	0.359 7	37.015	596.0	—2.0	1.6	
0.046 69	13.344	472.3	0.0	3.3		34.893	605.0	—3.5	1.6	
	4.7180	479.1	4.0	4.2	0.250 0	27.144	626.0	—0.5	1.5	
0.007 381	5.3097	478.1	—2.1	4.1		21.307	652.0	1.0	1.5	
	1.4480	305.6	4.5	4.6	0.156 6	13.816	665.0	3.1	2.8	
0.002 974 ^b	15.802	60.1	1.3	2.4	0.099 98	12.355	629.0	3.2	3.2	
	14.409	82.4	—5.6	2.7		10.227	647.0	1.7	3.2	
0.003 746	18.780	71.4	—0.6	2.4	0.039 51	3.2979	576.0	14.3	10.0	
	20.313	67.6	—0.4	2.4		3.0485	576.0	18.5	10.0	
0.004 886	24.635	72.9	1.9	2.5	0.003 462 ^b	16.451	86.8	—2.5	3.3	
	25.643	80.3	—1.8	2.6	0.003 539	17.564	81.0	—0.5	3.3	
0.005 945	30.097	77.6	—0.1	2.5	0.003 343	16.370	82.2	—1.8	2.7	
	28.541	81.1	—0.9	2.5	0.003 309	15.785	81.6	1.1	2.7	
0.006 354	31.633	78.1	2.2	2.0	0.004 868	23.300	94.7	—2.1	3.3	
	31.542	80.2	1.0	2.0	0.004 900	24.069	90.7	—0.9	3.3	
0.007 008	35.222	80.8	—0.1	1.8	0.003 534	17.189	81.1	1.4	2.1	
	36.508	80.8	—0.7	1.8	0.003 533	17.741	79.8	—0.5	2.1	
4.400	Gadolinium Nitrate					0.002 722	13.757	75.1	—2.8	1.5
	17.564	2363.5	1.4	2.4		0.002 734	11.580	86.5	2.0	1.5
	35.391*	2282.5	1.9	3.0	0.004 374	19.316	102.1	—3.7	1.8	
	16.451	2372.5	—1.0	2.4	0.004 506	19.981	102.5	—3.7	1.5	
	34.621*	2285.7	1.5	3.0	0.004 322	21.178	85.9	1.0	1.5	
	15.785	2019.7	1.3	2.0	0.005 752	28.026	97.5	—2.7	1.6	
	33.086*	1938.1	0.2	2.4	0.005 941	30.592	88.0	1.0	1.6	
3.952	16.370	2022.8	—5.4	2.0	0.010 07	49.787	103.6	2.6	2.0	
	33.432*	1940.6	—3.6	2.4	0.009 819	46.581	111.1	0.2	2.0	
3.622	24.069	1722.0	3.7	2.4		Terbium Nitrate				
	49.000*	1631.3	4.5	3.0	4.738	8.5020	3750.5	1.2	1.9	
	23.300	1731.4	—2.0	2.4		17.043*	3690.4	—3.2	2.7	
	48.679*	1636.7	0.1	3.0		8.7475	3755.5	—6.1	2.0	
3.238	17.741	1481.6	1.2	1.6						
	35.331*	1401.8	1.8	1.9						
	17.189	1483.5	2.6	1.6						
	35.343*	1402.4	1.1	1.9						

Table I. Continued

m_i	$10^4 m_f$	Expt — calcd					Exptl — calcd		
		$-\Delta H_{i,f}$ cal/mol	$\Delta H,$ cal/mol	$\sigma,$ cal/mol	m_i	$10^4 m_f$	$-\Delta H_{i,f},$ cal/mol	$\Delta H,$ cal/mol	$\sigma,$ cal/mol
4.502	9.2895	3509.9	7.6	2.0	0.090 93	13.754	729.8	0.7	2.6
	18.462*	3450.1	1.6	2.7		14.388	729.8	-3.7	2.5
	9.7226	3504.7	8.9	2.1	0.039 19	6.1935	619.9	-5.1	3.9
	19.478*	3449.3	-3.5	2.9		6.4255	617.9	-5.8	3.8
4.038	9.8811	3097.8	-4.3	1.9	0.001 704 ^b	8.502	60.1	4.4	2.9
	20.401*	3029.0	-7.0	2.7	0.001 846	9.289	59.8	6.0	3.0
	10.646	3092.7	-5.7	2.0	0.001 948	9.723	55.4	12.4	3.1
3.592	15.753	2668.3	1.9	2.5	0.002 040	9.881	68.8	2.8	2.9
	31.850*	2589.7	-1.3	3.5	0.003 185	15.753	78.7	3.1	3.8
	14.646	—	—	—	0.003 078	16.005	67.3	8.5	3.2
	31.834*	2585.3	3.1	3.0	0.002 939	13.585	80.8	5.4	3.3
3.249	16.005	2388.6	1.8	2.2	0.002 917	14.077	75.8	6.0	3.2
	30.784*	2321.3	-6.6	3.0	0.003 907	19.453	88.8	-1.9	3.6
	13.585	2399.8	7.0	2.1	0.003 915	19.704	77.8	8.0	3.6
	29.393*	2319.0	1.6	3.0	0.003 966	19.758	79.5	7.8	3.3
2.917	14.077	2405.1	-1.8	2.1	0.003 518	17.864	84.3	-2.4	2.6
	29.165*	2329.3	-7.7	3.0	0.003 441	17.170	82.2	0.9	2.6
	19.453	2109.0	5.2	2.4	0.004 633	22.691	103.6	-9.8	2.9
	39.066*	2020.2	7.1	3.3	0.005 465	27.113	110.5	-13.2	3.0
2.587	19.704	2105.2	7.6	2.5	0.005 906	29.749	105.9	-8.3	2.9
	39.148*	2027.4	-0.4	3.3	0.006 307	31.232	95.3	6.5	2.9
	20.100	1871.0	1.1	2.7	0.006 044	30.769	101.3	-4.3	2.6
	19.758	1873.8	0.2	2.2	0.006 108	31.197	90.4	6.5	2.6
2.274	39.663*	1794.3	-7.6	3.0	0.006 756	34.019	101.4	0.3	2.8
	17.864	1677.3	0.9	1.8	0.007 077	34.826	103.4	2.7	2.9
	35.181*	1593.0	3.3	2.4	0.006 933	34.872	102.0	0.6	2.7
	17.170	1688.7	-6.3	1.7	0.007 024	34.553	97.6	8.3	2.8
1.960	34.408*	1606.5	-7.2	2.4	0.006 212	30.994	98.7	1.7	2.4
	23.010	1466.9	-0.8	2.0	0.006 284	31.433	96.0	4.4	2.4
	22.691	1470.2	-2.4	2.0	0.004 612	23.266	85.3	4.9	1.8
	46.328*	1366.6	7.3	2.7					
1.705	26.190	—	—	—	4.539				
	53.834*	1221.6	1.0	2.2		7.5458	3184.3	-1.8	1.5
	27.113	1321.9	-4.3	2.1		15.273*	3123.1	-3.8	2.1
	54.654*	1211.5	8.8	2.8		7.5630	3180.3	2.0	1.5
1.440	29.280	—	—	—	4.323				
	58.121*	1097.7	1.3	2.1		15.522*	3118.9	-1.2	2.2
	29.749	1199.8	-5.6	2.1		9.5384	2968.4	0.4	1.8
	59.057*	1093.9	2.6	2.7		20.294*	2894.6	-0.5	2.6
1.215	31.241	—	—	—	3.925				
	62.004*	1011.5	0.1	2.0		11.124	2949.2	6.0	2.0
	31.232	1100.4	10.3	2.0		22.267*	2882.5	0.9	2.8
	63.073*	1005.1	3.8	2.7		12.948	2589.3	9.9	2.1
0.984 8	30.769	1053.5	-3.5	1.9	3.625				
	60.441*	952.2	0.9	2.4		28.111*	2509.6	3.6	3.2
	31.197	1043.5	4.8	1.9		12.104	2604.5	1.1	2.0
	61.084*	953.2	-1.8	2.4		26.479*	2530.4	-9.7	3.0
0.805 6	34.019	999.8	-3.4	2.0	3.193				
	67.564*	898.4	-3.6	2.5		16.118	2338.4	-5.8	2.3
	34.826	997.7	-4.4	2.0		32.610*	2251.5	-2.2	3.1
	70.774*	894.3	-7.1	2.6		15.557	2342.6	-6.3	2.2
0.662 7	34.872	964.6	-1.7	1.9	2.384				
	69.330*	862.6	-2.2	2.5		31.377*	2264.5	-10.1	3.0
	34.553	958.5	5.7	1.9		16.702	—	—	—
	70.237*	860.9	-2.7	2.5		29.988*	1924.5	3.8	1.8
0.488 5	30.994	935.1	2.0	1.7		18.804	—	—	—
	62.116*	836.4	0.3	2.2		37.608*	1365.4	0.4	1.8
	31.433	935.8	-0.6	1.7		20.098	1436.8	7.8	1.7
	62.844*	839.8	-5.0	2.2	2.210				
0.362 2	23.266	926.4	3.9	1.3		17.879	—	—	—
	46.116*	841.1	-1.0	1.7		36.147*	1371.7	-0.4	1.7
	27.626	906.8	2.7	1.5		22.393	1345.4	-7.2	1.8
	26.947	853.7	0.8	1.7		43.681*	1251.6	-1.0	2.3
0.251 3	27.217	856.8	-3.6	1.7		22.978	1329.5	5.7	1.8
	23.925	788.8	-0.7	1.4		46.285*	1231.1	11.0	2.4
0.161 5	23.414	791.0	-0.3	1.4		19.659	1358.2	-5.1	1.7
						42.523*	1259.0	-4.5	2.4
						20.111	1340.6	10.0	1.7
						42.144*	1251.6	4.2	2.3

Table I. Continued

m_i	$10^4 m_f$	Expt — calcd				m_i	$10^4 m_f$	Expt — calcd				
		$-\Delta H_{i,f}$, cal/mol	ΔH , cal/mol	σ , cal/mol				$-\Delta H_{i,f}$, cal/mol	ΔH , cal/mol	σ , cal/mol		
2.020	31.740	1204.3	-1.3	2.2	0.008 076	38.799	109.5	4.7	2.8			
	63.900*	1103.7	-3.2	2.9	0.007 046	35.563	102.0	1.3	2.4			
	30.734	1211.3	-4.1	2.2	0.007 203	36.333	104.3	-0.3	2.5			
	62.557*	1105.1	-1.2	2.9	0.004 946	25.335	88.5	2.7	1.8			
	1.752	20.793	1146.6	-1.0	1.4	0.005 043	25.137	89.7	5.4	1.8		
	41.975*	1054.2	0.9	1.9	0.003 881	19.584	86.0	0.1	2.2			
1.535	20.793	—	—	—								
	41.631*	1056.6	-0.3	1.5								
	31.024	1029.3	-4.1	1.9	5.027	13.846	4285.0	2.3	3.8			
	62.288*	928.3	-4.5	2.4		28.751*	4209.0	-3.2	4.6			
	30.795	—	—	—		14.153	4282.0	3.2	4.4			
	62.148*	923.8	0.3	1.9		16.614	4260.0	8.9	4.4			
1.209	39.180	912.5	3.2	2.0	4.564	12.989	3861.7	-3.1	3.1			
	74.544*	814.3	2.1	2.4		28.687*	3776.1	-5.0	3.8			
	37.758	918.6	2.3	2.0		13.293	3861.7	-5.3	3.1			
	74.633*	814.3	1.9	2.5		25.827*	3789.7	-5.5	3.8			
	1.045	43.768	870.7	1.6	2.1	4.131	16.378	3439.8	-5.3	3.4		
	87.056*	764.3	-1.9	2.7		33.710*	3349.8	-0.5	4.1			
0.860 2	43.371	—	—	—		17.331	3423.8	4.8	3.4			
	87.039*	761.6	0.8	2.1		33.074*	3347.4	4.4	4.1			
	38.799	865.1	0.3	2.0	3.724	16.104	3061.1	3.8	2.9			
	80.763*	755.5	-4.3	2.6		31.192*	2985.8	2.3	3.6			
	38.426	871.7	-4.9	2.0		16.851	3057.5	2.7	2.9			
	0.674 8	35.563	858.0	-1.3	1.7		33.501*	2975.6	3.1	3.6		
0.466 1	70.459*	756.0	-2.6	2.2	3.338	26.874	2657.0	5.8	4.3			
	36.333	855.1	-1.3	1.8		56.340*	2552.3	7.4	5.3			
	72.034*	750.9	-1.1	2.2		28.441	2658.9	-3.2	4.3			
	25.335	869.9	2.0	1.3		57.487*	2555.1	1.5	5.3			
	49.461*	781.4	-0.7	1.6	2.830	18.062	2276.7	-0.2	2.6			
	25.137	866.8	6.1	1.3		37.933*	2183.4	2.2	3.2			
0.357 1	50.428*	777.1	0.7	1.7		19.856	2266.5	-0.3	2.6			
	19.567	—	—	—		39.589*	2178.9	0.8	3.2			
	39.166*	793.2	-3.0	1.7	2.550	24.790	2017.3	0.7	2.9			
	19.584	874.6	3.0	1.2		48.414*	1926.6	1.6	3.5			
	38.809*	788.6	2.9	2.1		24.621	2025.9	-7.0	2.9			
	0.235 0	17.881	844.0	-4.9	1.5		50.723*	1925.2	-4.0	3.5		
0.157 4	17.804	845.2	-5.6	1.5	2.236	21.234	1805.9	-1.1	2.0			
	17.132	790.6	-4.9	1.8		36.881*	1735.5	0.2	2.4			
	17.076	789.5	-3.5	1.8		19.378	1817.9	-2.8	2.0			
	0.094 73	14.348	708.9	7.4	2.5		36.651*	1738.5	-1.9	2.4		
	14.373	710.3	5.8	2.5	1.958	21.013	1620.7	0.4	1.8			
	0.034 54	4.9441	591.3	10.2	4.0		39.038*	1542.2	0.7	2.3		
0.001 527 ^b	4.8552	588.5	14.1	4.1	1.685	19.360	1472.1	-2.1	2.2			
	4.8870	607.7	-5.5	4.0		50.581*	1346.8	-1.6	2.3			
	4.5640	612.2	-5.6	4.1	1.427	36.204	1261.7	1.5	2.6			
	7.546	61.2	2.0	2.3		74.511*	1150.2	3.7	3.2			
	7.563	61.5	3.1	2.3		37.100	1259.3	0.6	2.6			
	9.538	73.9	0.8	2.8		72.403*	1156.6	2.0	2.7			
0.002 227	11.124	66.7	5.1	3.0	1.210	31.159	1189.9	0.9	2.1			
	0.002 811	12.948	79.7	6.3		61.890*	1088.8	2.9	2.5			
	0.002 648	12.104	74.1	10.8		32.024	1185.0	2.2	2.1			
	0.003 261	16.118	86.9	-3.6		62.016*	1088.0	3.4	2.5			
	0.003 138	15.557	78.0	3.9	0.992 9	31.562	1113.6	-2.6	2.0			
	0.003 392	15.369	90.2	3.3		62.016*	1012.5	0.8	2.4			
0.003 712	18.028	89.7	-0.7	2.4		30.802	1114.6	-0.4	2.0			
	0.004 368	22.393	93.8	-6.2		65.157*	1003.4	2.0	2.4			
	0.004 628	22.978	98.5	-5.4	0.802 0	42.172	1011.6	0.6	2.2			
	0.004 252	19.659	99.1	-0.5		77.828*	916.7	0.0	2.7			
	0.004 214	20.111	89.1	5.7		45.874	998.3	1.7	2.2			
	0.006 390	31.740	100.6	2.0		79.210*	911.0	2.7	2.7			
0.006 256	30.734	106.2	-2.8	3.1	0.540 3	27.363	994.4	-2.5	1.5			
	20.793	92.4	-2.0	2.1		52.766*	901.2	0.0	1.8			
	31.024	101.0	0.5	2.6		26.430	999.0	-2.8	1.5			
	31.180	98.2	1.1	2.7		53.115*	899.7	0.5	1.8			
	37.758	104.3	0.3	2.7								
	0.008 706	43.768	106.4	3.6	3.0							

Table I. Continued

m_i	$10^4 m_f$	Expt					Expt			
		$-\Delta H_{i,f}$, cal/mol	— calcd		σ , cal/mol	m_i	$10^4 m_f$	$-\Delta H_{i,f}$, cal/mol	— calcd	
			ΔH , cal/mol	σ , cal/mol					ΔH , cal/mol	σ , cal/mol
0.491 5	23.455	996.3	-2.0	1.4	3.703	16.917	3264.5	-1.9	3.2	
	47.458*	905.0	-4.1	1.7		33.733*	3181.1	1.1	4.0	
	26.153	985.3	-4.0	1.4		16.753	3260.5	3.1	3.2	
	47.845*	901.8	-2.1	1.7		33.861*	3177.5	4.2	4.0	
0.359 8	20.812	950.0	5.5	1.2	3.288	35.450	2770.0	0.7	3.4	
	36.349*	883.0	3.1	1.4		17.927	2849.5	2.1	3.0	
	20.958	952.3	2.4	1.2		35.402*	2769.8	1.1	3.6	
	36.494*	882.4	3.1	1.4		17.842	2854.0	-1.9	3.0	
0.250 8	19.802	899.0	-1.6	1.3		35.438*	2770.4	0.4	3.6	
	19.634	904.0	-5.6	1.3	2.949	37.970	2437.0	2.5	3.5	
0.168 2	11.499	875.0	1.0	2.6		18.888	2524.0	0.0	2.8	
	11.485	871.0	5.1	2.6		37.442*	2440.0	1.4	2.9	
0.099 20	6.5434	809.0	4.0	3.6		18.602	2528.4	-2.8	3.1	
	6.4974	813.0	0.5	3.6		37.357*	2444.6	-2.9	3.8	
0.049 89	3.8809	693.0	4.7	10.0	2.570	20.052	2180.4	-5.8	2.5	
	3.1755	700.0	8.9	10.0		40.539*	2090.6	-3.0	2.7	
0.015 78	1.2996	487.0	19.3	10.0		20.530	—	—	—	
0.002 875 ^b	13.846	76.0	5.6	5.1		40.539*	2097.0	-9.4	2.9	
0.002 583	13.293	72.0	0.2	4.2	2.258	22.973	1897.8	-0.9	2.4	
0.002 869	12.989	85.6	1.8	4.2		43.639*	1811.8	3.2	3.0	
0.003 307	17.331	76.4	0.4	4.6		23.078	1895.2	1.2	2.4	
0.003 371	16.378	90.0	-4.7	4.6		43.441*	1812.1	3.5	3.0	
0.003 350	16.851	81.9	-0.4	4.0	1.969	24.800	1665.8	0.9	2.5	
0.003 119	16.104	75.3	1.5	4.0		51.710*	1565.3	3.8	3.0	
0.005 749	28.441	103.8	-4.7	5.9		24.701	1668.3	-1.2	2.5	
0.005 634	26.874	104.7	-1.7	5.9		51.725*	1568.2	0.8	3.0	
0.003 959	19.856	87.6	-1.1	3.5	1.712	31.248	1462.4	0.5	2.6	
0.003 793	18.062	93.3	-2.4	3.5		61.434*	1364.2	3.3	3.1	
0.005 072	24.621	100.7	-3.1	3.9		31.674	1460.0	1.2	2.6	
0.004 841	24.790	90.7	-0.9	3.9		62.284*	1362.9	2.4	3.1	
0.003 665	19.378	79.4	-0.9	2.7	1.422	32.376	1288.7	-0.1	2.4	
0.003 688	21.234	70.4	-1.3	2.7		66.929*	1188.4	-4.1	3.0	
0.003 904	21.013	78.5	-0.3	2.5		32.002	1291.7	-1.6	2.4	
0.005 058	19.360	125.3	-0.4	2.6		66.635*	1190.1	-5.1	3.0	
0.007 240	37.100	102.7	-1.4	3.1	1.209	28.101	1202.5	-0.1	1.8	
0.007 451	36.204	111.5	-2.1	3.5		52.882*	1114.7	1.9	2.2	
0.006 202	32.024	97.0	-1.2	2.8		28.037	1203.5	-0.8	1.8	
0.006 189	31.159	101.1	-2.0	2.8		52.867*	1114.3	2.3	2.2	
0.006 516	30.802	111.2	-2.4	2.7	1.005	42.602	1061.8	2.9	2.3	
0.006 202	31.562	101.1	-3.4	2.7		75.864*	973.7	3.3	2.8	
0.007 921	45.874	87.3	-1.0	3.0		42.042	1066.6	-0.1	2.3	
0.007 783	42.172	94.9	0.5	3.0		76.073*	974.3	2.2	2.8	
0.005 311	26.430	99.3	-3.3	2.0	0.813 8	29.976	1047.6	-1.3	1.7	
0.005 277	27.363	93.2	-2.5	2.0		56.295*	957.4	1.7	2.1	
0.004 784	26.153	83.5	-1.9	1.9	0.642 8	23.155	1026.8	-0.7	1.3	
0.004 746	23.455	91.3	2.2	1.9		44.636*	941.3	0.5	1.6	
0.003 649	20.958	69.9	-0.7	1.6		23.165	1026.7	-0.7	1.3	
0.003 635	20.812	67.0	2.4	1.6		44.449*	943.0	-0.6	1.6	
Erbium Nitrate										
5.456	10.278	5005.4	10.7	3.1		29.485	951.5	-0.8	1.4	
	20.867*	4935.0	11.6	3.8		50.737*	874.1	2.8	1.7	
5.179	11.499	4751.4	-9.4	3.3		28.079	957.1	-0.3	1.4	
	23.445*	4676.6	-7.4	4.1	0.351 6	50.325*	876.0	2.1	1.7	
	12.069	4753.9	-16.3	3.3		14.907	972.7	0.4	1.9	
	23.610*	4677.8	-9.4	4.1		27.405*	903.5	2.6	2.3	
4.848	13.032	4412.7	-0.7	3.4	0.254 6	25.990*	917.1	-4.6	2.3	
	26.348*	4332.5	4.4	4.2		9.8032	957.9	-1.6	2.4	
	13.148	4410.1	1.1	3.4	0.177 0	20.421*	888.0	-2.8	3.0	
	26.266*	4334.8	2.4	4.2		17.523	829.0	4.7	1.7	
4.452	14.869	4013.5	0.0	3.5	0.101 1	11.655	751.0	7.2	2.8	
	29.485*	3933.0	4.3	4.3		11.635	758.0	0.4	2.8	
	14.846	4010.3	3.4	3.5	0.038 30	2.9584	635.0	7.9	10.0	
	30.030*	3928.2	6.8	4.3		2.8291	637.0	8.2	10.0	
4.014	15.944	3573.9	1.6	3.3	0.002 087 ^b	10.278	70.4	-1.0	4.2	
	31.483*	3492.3	5.6	4.1	0.002 361	12.069	76.1	-6.8	4.5	

Table I. Continued

<i>m_i</i>	10 ⁴ <i>m_f</i>	Exptl					Expt				
		-Δ <i>H_{i,f}</i> , cal/mol	-calcd		<i>m_i</i>	10 ⁴ <i>m_f</i>	-Δ <i>H_{i,f}</i> , cal/mol	-calcd		Δ <i>H</i> , cal/mol	σ, cal/mol
			Δ <i>H</i> , cal/mol	σ, cal/mol				Δ <i>H</i> , cal/mol	σ, cal/mol		
0.002 344	11.499	74.8	-2.0	4.5	2.558	20.383	2200.8	-2.0	2.7		
0.002 627	13.148	75.3	-1.4	4.6		41.115*	2112.2	0.0	3.7		
0.002 635	13.032	80.2	-5.1	4.6		20.521	2191.4	6.7	2.6		
0.003 003	14.846	82.1	-3.4	4.8		39.768*	2116.5	0.2	3.5		
0.002 948	14.869	80.5	-4.3	4.8		20.571	2201.9	-4.1	2.8		
0.003 148	15.944	81.6	-4.1	4.5		20.554	2197.6	0.3	2.6		
0.003 386	16.753	83.0	-1.1	4.4		39.368*	2121.2	-3.1	3.4		
0.003 373	16.917	83.4	-3.0	4.4	2.249	22.281	1894.5	2.1	2.5		
0.003 544	17.842	83.6	-2.3	4.0		43.292*	1813.6	-0.8	3.2		
0.003 540	17.927	79.7	1.0	4.0		27.055	1876.6	-2.7	2.9		
0.003 736	18.602	83.8	0.1	4.2		52.876*	1786.5	-2.5	3.9		
0.003 744	18.888	84.0	-1.4	3.3		26.173	1877.4	0.5	3.4		
0.004 054	20.052	89.8	-2.9	3.1		26.999	—	—	—		
0.004 344	23.078	83.1	-2.3	3.3		52.662*	1801.0	-16.4	3.1		
0.004 364	22.973	86.0	-4.0	3.3		27.569	1873.4	-1.8	2.9		
0.005 172	24.701	100.1	-2.0	3.3		52.991*	1784.0	-0.3	3.8		
0.005 171	24.800	100.5	-2.9	3.3		26.639	1875.3	0.5	2.9		
0.006 228	31.674	97.1	-1.3	3.5		51.703*	1787.6	-0.3	3.8		
0.006 143	31.248	98.2	-2.8	3.5	1.961	27.636	1627.9	-1.4	3.2		
0.006 663	32.002	101.6	3.5	3.3		26.861	1627.1	2.9	2.5		
0.006 693	32.376	100.3	4.0	3.3		51.627*	1539.2	3.6	3.2		
0.005 287	28.037	89.2	-3.1	2.5	1.696	33.977	1397.1	7.0	2.7		
0.005 288	28.101	87.8	-1.9	2.5		64.222*	1308.6	4.7	3.4		
0.007 607	42.042	92.3	-2.3	3.1		35.358	1396.3	2.6	2.7		
0.007 586	42.602	88.1	-0.4	3.1		65.840*	1310.4	-1.0	3.4		
0.005 630	29.976	90.2	-2.9	2.3	1.445	30.025	1260.9	1.5	2.1		
0.004 445	23.165	83.7	-0.1	1.8		53.074*	1181.0	3.8	2.5		
0.004 464	23.155	85.5	-1.2	1.8		29.340	1259.8	5.5	2.0		
0.005 032	28.079	81.1	-2.5	1.9		51.824*	1184.2	4.1	2.4		
0.005 074	29.485	77.4	-3.6	1.9	1.210	37.173	1118.4	-2.9	2.2		
0.002 599	12.341	83.8	-5.3	2.5		62.244*	1043.4	-2.2	2.5		
0.002 741	14.907	69.2	-2.2	2.5		40.501	1104.5	-0.6	2.3		
0.002 042	9.803	69.9	1.2	3.3		65.073*	1034.0	0.4	2.6		
Thulium Nitrate											
6.028	9.9901	5994.5	7.7	3.6		0.997 8	26.814	1073.3	-1.9	1.6	
	20.668*	5931.7	-0.1	5.3			47.537*	995.3	0.6	1.9	
	11.337	5992.0	-0.7	4.0			30.715	1055.1	-0.4	1.8	
	22.182*	5921.1	2.6	5.4	0.819 4		57.176*	975.6	-6.8	2.3	
5.499	10.539	5450.9	-21.4	3.4			26.151	1021.6	-4.4	1.4	
	21.244*	5389.8	-29.4	4.9			25.407	1018.9	1.7	1.3	
	10.744	5415.6	12.2	3.5			42.479*	954.8	-0.2	1.8	
	21.453*	5350.7	8.6	4.8			26.430	1017.2	-1.3	1.9	
5.016	10.707	4913.5	2.7	3.2			27.149	—	—	—	
	21.582*	4841.0	5.7	4.4			44.975*	941.6	5.0	1.6	
	10.514	—	—	—			26.223	1021.0	-4.1	1.4	
	19.107*	4857.0	3.1	2.9			43.681*	953.4	-2.7	1.8	
4.412	12.980	4252.5	-2.7	3.3	0.616 4		25.787	1019.0	-0.1	1.4	
	26.325*	4167.2	7.4	4.6			44.090*	947.7	1.7	1.7	
	13.491	4242.6	3.5	3.4			26.343	965.7	-4.5	1.4	
	26.724*	4173.1	-0.3	4.7			48.515*	881.3	-0.6	1.8	
3.997	15.334	3779.9	-1.1	3.4	0.479 9		27.184	957.6	-0.2	1.5	
	15.470	3783.7	-5.8	3.4			50.195*	873.6	2.1	1.8	
	30.303*	3694.1	8.4	4.6			22.600	—	—	—	
3.765	17.102	3513.0	-2.6	3.5			40.151*	863.6	5.7	1.9	
	32.987*	3427.5	6.9	4.6			22.758	936.3	4.0	1.1	
	17.555	3497.8	9.9	3.6			40.579*	861.0	6.8	1.7	
	34.306*	3418.9	10.4	4.8			23.041	938.4	0.5	1.6	
3.246	19.065	2934.9	-7.8	3.2	0.360 2		23.958	934.7	-0.3	1.2	
	35.783*	2857.5	-5.6	4.1			42.614*	860.5	0.6	1.7	
	17.536	2937.9	-2.0	3.1			19.401	921.5	-5.5	1.3	
	35.105*	2856.0	-1.6	4.2			34.939*	845.8	0.1	2.4	
2.906	19.530	2558.7	0.8	2.9			19.858	913.5	0.0	1.3	
	37.661*	2482.2	-2.1	3.8			34.408*	850.7	-2.8	2.5	
	19.037	2560.7	1.6	2.8			19.651	914.7	0.0	1.3	
	37.115*	2485.0	-2.9	3.8			19.700	912.3	2.1	1.2	
							35.612*	840.5	2.9	2.3	

Table I. Continued

m_i	$10^4 m_f$	Expt					Exptl		
		$-\Delta H_{i,f}$, cal/mol	ΔH_i , cal/mol	σ , cal/mol	m_i	$10^4 m_f$	$-\Delta H_{i,f}$, cal/mol	ΔH_i , cal/mol	σ , cal/mol
							—	calcd	—
0.214 4	14.041	871.9	-7.1	2.1	5.761	7.1650	5915.7	12.3	2.6
	25.491*	805.5	-4.6	3.5		14.448*	5874.8	-5.2	3.6
	14.023	867.1	-2.2	2.1		7.0983	5943.9	-15.2	2.5
	25.720*	800.5	-0.7	3.5	5.306	6.8908	5456.1	-6.6	2.3
	11.831	879.9	0.8	2.3		7.1886	5441.8	4.7	2.4
	21.565*	821.7	-1.5	3.8		14.595*	5397.3	-9.9	3.4
	11.747	885.9	-4.5	2.4	4.816	7.8896	4876.8	10.8	2.3
	20.962*	820.1	3.2	3.9		15.670*	4829.0	-0.5	3.2
0.161 7	17.666	787.8	2.7	1.8	4.445	8.5378	4435.0	11.2	2.3
	16.558	794.1	3.1	1.9		17.359*	4382.2	0.8	3.3
	14.732	803.1	5.8	2.2		9.1106	4438.6	2.5	2.4
0.091 31	13.213	709.4	-2.5	2.7		18.202*	4383.2	-5.0	3.4
	11.191	723.9	-1.8	3.0	3.994	10.749	3884.6	-0.9	2.5
	11.419	720.9	-0.6	2.9		21.081*	3821.4	-2.4	3.4
0.034 59	3.4955	595.1	8.6	4.2		10.821	3876.9	6.2	2.5
	4.1489	589.4	4.5	4.1		21.075*	3825.9	-6.9	3.4
0.002 067 ^b	9.990	62.8	7.8	5.7	3.576	12.571	3368.3	-3.7	2.6
0.002 218	11.337	70.9	-3.4	5.9		25.352*	3301.4	-8.3	3.6
0.002 124	10.539	61.1	8.0	5.2		12.573	3365.7	-1.1	2.6
0.002 145	10.744	64.8	3.7	5.2		25.781*	3300.5	-9.4	3.7
0.002 158	10.707	72.4	-2.9	4.8	3.226	12.301	2949.5	-0.4	2.3
0.002 633	12.980	85.4	-10.3	5.0		27.112*	2872.2	-4.3	3.5
0.002 672	13.491	69.5	3.8	5.1		14.690	2940.6	-7.9	2.6
0.003 030	15.470	89.6	-14.2	5.0		29.104*	2869.9	-10.4	3.5
0.003 299	17.102	85.5	-9.5	5.0	2.552	19.523	2149.2	4.6	2.5
0.003 431	17.555	78.9	-0.5	5.3		39.467*	2070.6	0.2	3.5
0.003 578	19.065	77.4	-2.2	4.5		19.495	—	—	—
0.003 511	17.536	81.9	-0.4	4.6		40.125*	2067.4	1.2	2.9
0.003 766	19.530	76.6	2.8	4.2	2.249	22.166	1839.3	2.0	2.4
0.003 711	19.037	75.7	4.5	4.2		44.468*	1755.0	1.0	3.3
0.004 112	20.383	88.7	-2.1	4.0		21.961	1841.1	1.2	2.4
0.003 977	20.521	74.9	6.4	3.8		45.084*	1752.2	1.9	3.4
0.003 937	20.554	76.4	3.4	3.7	1.963	25.592	1573.0	1.0	2.4
0.004 329	22.281	80.9	2.9	3.5		53.269*	1476.8	2.9	3.4
0.005 288	27.055	90.1	-0.2	4.2		26.670	1567.4	1.8	2.5
0.005 299	27.569	89.3	-1.4	4.2		54.169*	1476.1	1.2	3.4
0.005 170	26.639	87.7	0.7	4.1	1.687	29.920	1345.3	3.1	2.4
0.005 163	26.861	87.9	-0.7	3.6		60.104*	1250.9	4.0	3.1
0.006 422	33.977	88.5	2.3	3.7		29.858	1346.6	2.0	2.4
0.006 584	35.358	85.9	3.6	3.8		60.830*	1248.4	4.8	3.2
0.005 307	30.025	79.9	-2.3	2.7	1.461	30.091	1200.2	6.6	2.1
0.005 182	29.340	75.7	1.3	2.7		58.814*	1111.3	5.9	2.7
0.006 224	37.173	74.9	-0.8	2.8		29.425	1212.5	-3.0	2.1
0.006 507	40.501	70.4	-1.0	2.9		58.915*	1118.0	-1.0	2.7
0.004 754	26.814	78.0	-2.5	2.1	1.211	31.112	1082.8	-3.5	2.0
0.005 718	30.715	79.5	6.4	2.5		62.800*	984.9	-0.8	2.6
0.004 248	25.407	64.1	1.9	1.9		31.036	1081.8	-2.2	2.0
0.004 368	26.223	67.6	-1.5	1.9		63.777*	983.3	-1.5	2.6
0.004 409	25.787	71.3	-1.9	1.9	1.015	33.021	1002.2	-3.4	1.9
0.004 852	26.343	84.4	-3.9	1.9		65.486*	905.7	-1.1	2.5
0.005 019	27.184	84.0	-2.3	2.0		33.457	1000.3	-3.1	1.9
0.004 058	22.758	75.3	-2.8	1.8		65.814*	905.7	-1.8	2.5
0.004 261	23.958	74.2	-0.9	1.8	0.836 2	35.211	943.1	-2.7	1.8
0.003 494	19.401	75.7	-5.5	2.5		69.056*	855.8	-9.6	2.6
0.003 441	19.858	62.8	2.8	2.6		35.344	939.0	0.9	1.9
0.003 486	19.651	63.7	4.8	2.5		70.999*	845.6	-3.7	2.5
0.003 561	19.700	71.8	-0.8	2.4	0.689 4	36.809	—	—	—
0.002 549	14.041	66.3	-2.4	3.7		73.671*	798.8	4.5	1.9
0.002 572	14.023	66.7	-1.7	3.7		36.230	906.7	-2.9	2.3
0.002 156	11.831	58.2	2.4	4.0		36.755	900.0	1.9	1.9
0.002 096	11.747	65.8	-7.8	4.1		35.567	908.5	-2.4	1.9
	Ytterbium Nitrate					72.538*	808.2	-2.5	2.5
6.650	5.5780	6792.0	1.7	2.4	0.497 5	31.381	880.0	0.4	1.6
	11.806*	6748.0	-11.6	3.5		60.245*	789.1	4.1	2.0
	6.0643	6784.4	3.7	2.5		31.983	—	—	—
						66.482*	776.4	2.1	1.7

Table I. Continued

<i>m_i</i>	10 ⁴ <i>m_f</i>	Exptl					Exptl				
		—calcd		σ , cal/mol	<i>m_i</i>	10 ⁴ <i>m_f</i>	—calcd		σ , cal/mol		
		—Δ <i>H_{i,f}</i> , cal/mol	Δ <i>H</i> , cal/mol				Δ <i>H</i> , cal/mol	σ, cal/mol			
0.373	2	21.696	886.1	2.7	1.4	4.060	17.065	3912.6	2.5	3.8	
		23.207	883.1	-1.7	1.2		34.152*	3833.2	1.5	4.7	
		45.225*	801.0	-2.1	1.6		18.139	3898.0	10.8	3.8	
		22.220	883.6	2.6	1.1		31.900*	3837.7	5.7	4.7	
		43.736*	801.5	1.9	1.6	3.644	32.707	3306.0	-1.7	3.4	
		22.299	884.8	1.0	1.2		16.802	3383.2	-2.4	3.2	
		44.650*	800.8	-0.2	1.6		31.438*	3312.2	-2.9	3.9	
0.233	4	25.248	799.4	3.1	1.5	2.928	14.228	2515.6	-0.8	2.2	
		26.043	801.3	-2.4	1.5		29.463*	2435.5	-0.5	2.7	
0.159	6	21.737	751.5	-0.1	1.2		15.960	2517.3	-13.8	2.2	
		23.925	743.8	-3.0	1.3		30.151*	2441.3	-9.2	2.4	
0.089	00	14.059	681.7	-2.3	2.7	2.596	47.403	1997.0	4.4	4.4	
		13.658	687.0	-4.9	2.7		25.110	2080.1	3.7	3.8	
0.039	93	6.6410	578.5	-3.3	3.9		47.486*	1997.1	4.0	4.6	
		6.8633	576.4	-3.6	3.8	2.260	19.678	1778.7	-2.8	1.9	
0.001	181 ^b	5.578	44.0	13.3	3.8		35.784*	1705.2	-0.8	2.3	
		0.001 445	7.165	40.9	17.5		19.616	1774.7	1.5	1.9	
		0.001 460	7.189	44.5	14.6		36.228*	1700.0	2.8	2.3	
		0.001 567	7.890	47.8	11.3	3.5	21.041	1585.3	-0.8	1.9	
		0.001 736	8.538	52.8	10.3		39.363*	1506.4	1.2	2.3	
		0.001 820	9.111	55.4	7.5		20.539	1580.1	7.0	1.9	
		0.002 108	10.749	63.2	1.5		40.145*	1499.6	5.4	2.3	
		0.002 108	10.821	50.9	13.2	3.7	34.059	1269.3	3.6	2.4	
		0.002 535	12.571	66.9	4.6		67.289*	1172.3	3.5	3.0	
		0.002 578	12.573	65.2	8.2		33.466	1273.3	1.9	2.4	
		0.002 711	12.301	77.3	3.9		68.013*	1170.8	3.3	3.0	
		0.002 910	14.690	70.6	2.7	3.8	20.485	1176.0	-0.8	1.5	
		0.003 947	19.523	78.6	4.4		42.628*	1085.4	-0.8	1.8	
		0.004 447	22.166	84.4	0.9		20.304	1175.9	0.3	1.5	
		0.004 508	21.961	88.9	-0.7		43.639*	1078.4	2.9	1.8	
		0.005 327	25.592	96.2	-1.8	3.6	25.735	1046.4	-3.2	1.5	
		0.005 417	26.670	91.4	0.6		50.141*	958.9	-3.3	1.8	
		0.006 010	29.920	94.3	-0.8		24.890	1049.4	-2.3	1.5	
		0.006 083	29.858	98.2	-2.7		49.393*	957.8	0.0	1.8	
		0.005 881	30.091	88.8	0.8	3.0	0.991 7	33.051	955.6	-1.3	1.8
		0.005 891	29.425	94.5	-2.0		65.659*	856.4	0.7	2.1	
		0.006 280	31.112	97.9	-2.7		33.652	953.8	-1.8	1.8	
		0.006 378	31.036	98.5	-0.7		65.659*	857.4	-0.3	2.1	
		0.006 549	33.021	96.5	-2.3	2.7	0.813 5	29.528	928.6	-0.8	1.6
		0.006 581	33.457	94.6	-1.3		59.521*	830.6	0.9	1.9	
		0.006 906	35.211	87.3	6.9		31.136	919.2	2.0	1.6	
		0.007 100	35.344	93.4	4.5		60.949*	825.2	2.7	1.9	
		0.007 254	35.567	100.3	0.1	2.7	0.640 3	25.150	918.1	-2.7	1.4
		0.006 024	31.381	91.7	-3.7		54.258*	812.6	0.9	1.7	
		0.004 523	23.207	82.1	0.5		27.794	905.2	-1.7	1.4	
		0.004 374	22.220	82.0	0.8		56.130*	808.6	-0.1	1.7	
		0.004 465	22.299	84.0	1.2		22.043	901.2	0.2	1.1	
		Lutetium Nitrate					41.719*	820.7	1.2	1.4	
6.792		5.7936	7150.0	21.5	3.5		23.785	891.9	0.9	1.1	
		5.3917	7190.6	-14.3	3.1		42.263*	819.1	1.0	1.4	
		15.508*	7090.2	-0.5	3.7	0.359 9	17.090	893.8	0.4	1.8	
5.804		9.1264	6092.5	2.7	3.0		32.013*	816.3	5.9	2.1	
		16.048*	6049.8	-5.9	3.7		13.271	917.0	2.0	2.0	
		8.3752	6104.1	-2.0	3.0	0.246 6	18.404	838.0	-3.1	1.5	
		16.573*	6037.6	3.1	3.7		17.231	842.0	-0.3	1.5	
5.482		7.4857	5744.0	3.2	3.1	0.160 4	18.430	839.0	-4.3	1.5	
		7.3875	5751.2	-3.0	2.7		8.8387	833.0	2.3	3.0	
		16.048*	5683.8	-3.5	3.3		11.022	810.0	4.4	3.0	
5.056		8.3694	5248.1	-12.8	2.7	0.101 6	6.4212	760.0	13.6	3.6	
		16.859*	5177.5	-5.5	3.3		6.9485	764.0	3.9	3.6	
4.872		17.148	4930.3	15.2	5.1	0.047 95	3.7210	657.0	2.9	10.0	
		35.212*	4844.5	17.1	6.2		3.3856	656.0	9.1	10.0	
4.553		13.293	4561.8	9.9	3.8	0.008 001	0.7894	366.0	21.8	10.0	
		28.048*	4483.7	7.7	4.7		0.7742	330.0	58.3	10.0	
		13.935	4556.3	10.9	3.8	0.001 551 ^b	5.392	100.4	-13.7	4.1	
		28.505*	4475.6	13.8	4.7						

Table I. Continued

m_i	$10^4 m_f$	Exptl —calcd				m_i	$10^4 m_f$	Exptl —calcd			
		$\Delta H_{i,f}$, cal/mol	ΔH_i , cal/mol	σ , cal/mol				$\Delta H_{i,f}$, cal/mol	ΔH_i , cal/mol	σ , cal/mol	
0.001 657	8.375	66.5	-5.0	4.0	0.003 936	21.041	78.9	-2.1	2.5		
0.001 605	9.126	42.7	8.6	4.0	0.006 801	33.466	102.5	-1.4	3.3		
0.001 605	7.388	67.4	0.5	3.7	0.006 729	34.059	97.0	0.1	3.3		
0.001 686	8.369	70.6	-7.3	3.6	0.004 364	20.304	97.5	-2.6	2.0		
0.003 521	17.148	85.8	-1.9	6.9	0.004 263	20.485	90.6	0.1	2.0		
0.002 850	13.935	80.7	-2.9	5.1	0.004 939	24.890	91.6	-2.2	2.0		
0.002 805	13.293	78.1	2.2	5.1	0.005 014	25.735	87.5	0.1	2.0		
0.003 190	18.139	60.3	5.0	5.1	0.006 566	33.652	96.4	-1.5	2.4		
0.003 415	17.065	79.4	1.0	5.1	0.006 566	33.051	99.2	-2.0	2.4		
0.003 144	16.802	71.0	0.4	4.3	0.006 095	31.136	94.0	-0.7	2.1		
0.003 015	15.960	76.0	-4.6	2.7	0.005 952	29.528	98.0	-1.7	2.1		
0.002 946	14.228	80.1	-0.2	3.0	0.005 613	27.794	96.6	-1.6	1.9		
0.004 749	25.110	83.0	-0.3	5.1	0.005 426	25.150	105.5	-3.7	1.9		
0.003 623	19.616	74.7	-1.3	2.6	0.004 226	23.785	72.8	-0.1	1.5		
0.003 578	19.678	73.5	-2.0	2.6	0.004 172	22.043	80.5	-0.9	1.5		
0.004 014	20.539	80.5	1.7	2.5	0.003 201	17.090	77.5	-5.5	2.4		

^a For a starred sample $f = 3$ and its corresponding $f = 2$ value (unstarred) is given immediately above. ^b For each salt, all entries above this point are $\Delta H_{1,2}$ or $\Delta H_{1,3}$ values, the rest are $\Delta H_{3,2}$ values.

The heat of dilution data for each salt were fitted to

$$\Delta H_{i,f} = \sum_j A_j (m_j^{p_j} - m_i^{p_j}) \quad (6)$$

using statistical weights. In this equation i represents the initial molality and f the final molality. For the rare earth nitrates, $A_1 = 6990$ is the Debye-Hückel limiting slope. This value was obtained (4) using various sources of dielectric constant data and it appears to be uncertain to about $\pm 5\%$. The least-squares parameters from eq 6 can be used to generate values of ϕ_L from

$$\phi_L = \sum_j A_j m_j^{p_j} \quad (7)$$

where no subscript is needed for m since these heats are now relative to the infinitely dilute solution.

Power series in $m^{1/4}$ were found to work best in eq 6 for the earth nitrates, provided the p_j 's were not required to form a consecutive sequence. All possible fits with six terms between $m^{3/4}$ and $m^{16/4}$ were performed. The powers finally chosen to represent the data were picked for giving good fits and so that each salt would have the most powers in common. The χ^2 values for the fits were also used as guides in picking the power series finally chosen to represent the data. The experimental heat data, and the difference between the experimental and calculated heats, are given in Table I. The highest concentration for each salt is the saturated solution.

The relative partial molal enthalpies of the solute

$$\bar{L}_2 = (\partial(m\phi_L)/\partial m)_{T,P,n_1} \quad (8)$$

and solvent

$$\bar{L}_1 = \frac{-m^2 M_1}{1000} \left(\frac{\partial \phi_L}{\partial m} \right)_{T,P,n_1} \quad (9)$$

can be calculated from eq 7. These quantities are needed in order to calculate the temperature derivatives of the activity coefficients and water activities.

If samples of the hydrated crystals are dissolved in water to form a solution,

$$q' = n'[\phi_L(m_2) - \bar{L}_2] = n' \Delta H_{x,2} \quad (10)$$

where \bar{L}_2 is the heat of solution to form an infinitely dilute solution

Table II. Heats of Solution of Some Rare Earth Nitrate Hydrates at 25 °C

Hydrate	$10^4 m_f$	$-\Delta H_{x,f}$, cal/mol	$\phi_L(m_f)$, cal/mol	\bar{L}_2 , cal/mol
$\text{La}(\text{NO}_3)_3 \cdot 6\text{H}_2\text{O}$	10.936	-4674.4	204.0	-4470.4
	26.184*	-4773.7	297.1	-4476.6
	13.381	-4678.4	223.0	-4455.4
	28.377*	-4772.9	307.2	-4465.7
$\text{Nd}(\text{NO}_3)_3 \cdot 6\text{H}_2\text{O}$	11.827	-4200.0	204.7	-3995.3
	12.917	-4214.1	212.6	-4001.5
$\text{Gd}(\text{NO}_3)_3 \cdot 6\text{H}_2\text{O}$	16.744	—	—	—
	32.058*	-3340.2	312.3	-3027.9
	14.501	-3262.6	225.2	-3037.4
	31.968*	-3341.3	311.9	-3029.4
$\text{Ho}(\text{NO}_3)_3 \cdot 6\text{H}_2\text{O}$	12.902	—	—	—
	28.249*	-1340.1	303.6	-1036.6
	12.996	-1253.1	218.1	-1035.0
	24.206*	-1320.8	284.7	-1036.2
$\text{Er}(\text{NO}_3)_3 \cdot 6\text{H}_2\text{O}$	15.579	-798.8	233.5	-565.3
	33.074*	-891.6	319.7	-571.9
	18.550	-820.6	251.6	-569.1
	35.260*	-897.5	328.1	-569.4
$\text{Lu}(\text{NO}_3)_3 \cdot 5\text{H}_2\text{O}$	11.269	—	—	—
	26.512*	2483.9	291.4	2775.2
	11.937	2571.9	207.9	2779.9
	Average			2778 ± 2

^a For a starred sample $f = 3$ and its corresponding $f = 2$ value (unstarred) is given immediately above.

per mole of salt, q' is the heat of solution of the sample and the other symbols have the same meaning as above. If a second sample is added to the first solution,

$$q' + q'' = (n' + n'')[\phi_L(m_3) - \bar{L}_2] = (n' + n'')\Delta H_{x,3} \quad (11)$$

where q'' is this second heat of solution. Using ϕ_L values calculated from eq 7, based on the experimental heat of dilution

Table III. Parameters for Equations 6 and 7^a

Salt	P_2 A_2	P_3 A_3	P_4 A_4	P_5 A_5	P_6 A_6	P_7 A_7
$\text{La}(\text{NO}_3)_3$	1.00 -32 256.750	1.25 41 877.6139	1.75 -34 910.5211	2.00 20 602.5901	2.75 -1 694.94423	3.25 240.06052
$\text{Pr}(\text{NO}_3)_3$	1.00 -38 190.618	1.25 64 588.4396	1.50 -38 613.3646	2.00 6 386.5588	3.00 -381.46265	3.75 34.517854
$\text{Nd}(\text{NO}_3)_3$	1.00 -42 867.795	1.25 77 861.7362	1.50 -50 553.4184	2.00 10 677.8261	2.75 -2 131.75308	3.00 762.84252
$\text{Sm}(\text{NO}_3)_3$	1.00 -56 611.355	1.25 122 852.7997	1.50 -99 352.3369	2.00 51 998.8964	2.25 -31 194.7115	2.50 5875.23604
$\text{Gd}(\text{NO}_3)_3$	1.00 -40 307.236	1.25 69 831.3558	1.50 -42 102.4691	2.00 6 742.7600	3.25 -484.16203	3.50 213.06066
$\text{Tb}(\text{NO}_3)_3$	1.00 -34 591.560	1.25 56 270.9110	1.50 -31 747.6025	2.00 4 376.9553	3.75 -136.033881	4.00 68.458381
$\text{Dy}(\text{NO}_3)_3$	1.00 -37 311.223	1.25 67 721.7929	1.50 -44 607.9683	2.00 10 262.1880	2.50 -1 695.74648	4.00 9.212981
$\text{Ho}(\text{NO}_3)_3$	1.00 -37 331.209	1.25 67 668.4967	1.50 -44 314.5013	2.00 9 700.1017	2.75 -1 998.28716	3.00 716.49916
$\text{Er}(\text{NO}_3)_3$	1.00 -41 318.993	1.25 83 725.1907	1.50 -64 686.3315	2.00 29 628.2407	2.25 -13 685.5629	2.75 764.11612
$\text{Tm}(\text{NO}_3)_3$	1.00 -40 532.695	1.25 77 329.4719	1.50 -53 296.0584	2.00 12 639.2692	2.75 -2 763.43574	3.00 998.78016
$\text{Yb}(\text{NO}_3)_3$	1.00 -46 803.234	1.25 102 854.4338	1.50 -86 229.2843	2.00 48 349.3896	2.25 -29 349.2141	2.50 5494.64542
$\text{Lu}(\text{NO}_3)_3$	1.00 -40 512.376	1.25 76 029.7792	1.50 -51 028.6371	2.00 10 994.4242	2.75 -1 388.03073	3.25 189.96374

^a $P_1 = 0.50$, $A_1 = 6990.00$ for all salts.

data, \bar{L} -values were calculated and these are given in Table II. The least-squares coefficients for eq 6 and 7 are listed in Table III.

The random error in each measurement was found to depend on the heat evolved, q , for that measurement. The estimated standard deviation for each ΔH measurement, σ , is listed in Table I. These errors are about 10 cal mol⁻¹ in ΔH when q is less than 0.3 cal. They reach a minimum of 1.1 cal mol⁻¹ when $q = 1.5$ cal, and then increase to about 4.5 cal mol⁻¹ for larger heats. These estimated errors were used to assign weighting factors for eq 6. The standard deviations for the least-squares fits finally chosen are 2.4–4.8 cal mol⁻¹, which indicates that systematic deviations of the fits from the original data must be small. This is illustrated in Figure 1 where the difference between the experimental and calculated values of ΔH is shown as a function of the square root of the initial molality for $\text{Ho}(\text{NO}_3)_3$.

In addition to the random errors, there is a possible systematic error of about 0.2% in ΔH and ϕ_L due to the calorimeter calibration (14 cal mol⁻¹ or less; decreasing with concentration). The errors in ΔH and ϕ_L due to the stock solution concentration uncertainty range from 8 cal mol⁻¹ at high concentrations to becoming almost negligible at low concentrations. These errors are systematic errors for all of the dilutions from the same stock solution, but they are absolute errors relative to the saturated solution. By comparison of various fits to the same data set, the extrapolations to infinite dilution were estimated to result in errors for ϕ_L and ΔH of 10 cal mol⁻¹ or less.

A random variable technique was used to estimate the errors in \bar{L}_1 and \bar{L}_2 due to random errors in ΔH . In Table IV the values of ϕ_L , $(d\phi_L/dm^{1/2})$, \bar{L}_1 , and \bar{L}_2 and their errors (standard deviations) are listed for $\text{La}(\text{NO}_3)_3$. The errors in ϕ_L are essentially those in ΔH . The method used to estimate these errors is given in detail elsewhere (4), along with a listing of the error values for the other rare earth nitrates. It should be noted that these errors are random errors only; they do not take into account any systematic errors that may be present.

Discussion

In Figure 2 the ϕ_L values for La, Nd, Tb, and Lu nitrate solutions are shown as a function of the square root of the molality. At high concentrations the ϕ_L curves for the rare earth nitrates increase

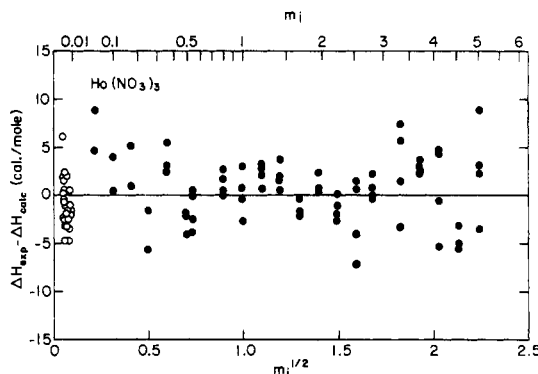


Figure 1. Differences between experimental and calculated $\Delta H_{i,f}$ values: open circles are $\Delta H_{3,2}$ values, closed circles are $\Delta H_{1,2}$ and $\Delta H_{1,3}$.

with the atomic number of the rare earth, whereas at lower concentrations some crossovers occur. Except for dilute solutions, the ϕ_L values for the nitrate salts are much lower than for the corresponding rare earth perchlorates (16).

In Figure 3 the \bar{L}_2 values are shown for the same four salts. The \bar{L}_2 curves rise more steeply than the ϕ_L curves at high concentrations. The crossovers occur at higher concentrations for ϕ_L than for \bar{L}_2 . This is due to the integral nature of ϕ_L , since the behavior at lower concentrations contributes to ϕ_L at higher concentrations while \bar{L}_2 represents the actual behavior of the system at the concentration of interest. In Figure 4 the \bar{L}_1 curves for these same salts are shown as a function of the molality.

All of the rare earth perchlorates saturate out between 4.60 and 4.76 m at 25 °C. The values of ϕ_L range from 6.5 to 7.5 kcal for these saturated solutions. At 4.6 m, the rare earth nitrates have ϕ_L values between 1.8 and 4.6 kcal. The rare earth nitrates liberate much less heat, upon dilution from high concentrations, than the corresponding rare earth perchlorates, and the nitrate heats also show larger differences across the rare earth series. The nitrate ϕ_L values would be expected to be larger than for the corresponding perchlorate salts, if anion size differences were the only significant changes between these systems. This occurs

Table IV. Thermodynamic Properties and Errors for $\text{La}(\text{NO}_3)_3$ Solutions at 25 °C

Molality	ϕ_L , cal/mol	$d\phi_L/dm^{1/2}$	$-\bar{L}_1$, cal/mol	\bar{L}_2 , cal/mol
4.608	1842.2 ± 3.1	2215.9 ± 23.2	197.4 ± 2.1	4220.6 ± 25.1
4.456	1765.0 ± 2.6	2111.7 ± 15.6	178.9 ± 1.3	3993.8 ± 16.7
4.000	1545.9 ± 3.4	1850.5 ± 4.1	133.35 ± 0.30	3396.4 ± 5.4
3.606	1369.3 ± 1.8	1646.6 ± 4.4	101.56 ± 0.27	2932.7 ± 4.5
3.239	1216.0 ± 1.9	1441.7 ± 3.8	75.70 ± 0.20	2513.3 ± 3.9
2.893	1084.4 ± 1.6	1216.7 ± 2.5	53.93 ± 0.11	2119.1 ± 2.7
2.557	973.3 ± 1.7	960.6 ± 2.2	35.379 ± 0.081	1741.4 ± 2.4
2.092	857.9 ± 1.3	548.7 ± 2.4	14.954 ± 0.066	1254.7 ± 2.2
1.960	835.4 ± 1.4	423.4 ± 2.3	10.466 ± 0.058	1131.8 ± 2.1
1.694	806.4 ± 1.9	169.3 ± 2.1	3.363 ± 0.041	916.6 ± 2.4
1.341	805.6 ± 2.2	-144.5 ± 2.3	-2.021 ± 0.032	722.0 ± 2.6
1.208	817.2 ± 1.5	-245.0 ± 2.5	-2.930 ± 0.030	682.6 ± 2.0
1.000	848.0 ± 1.7	-367.7 ± 2.6	-3.312 ± 0.023	664.2 ± 2.1
0.810 1	888.3 ± 2.0	-426.4 ± 2.3	-2.801 ± 0.015	696.4 ± 2.3
0.639 7	-931.1 ± 2.1	-415.4 ± 2.2	-1.914 5 ± 0.010 0	765.0 ± 2.3
0.489 1	969.2 ± 1.8	-332.0 ± 2.7	-1.022 9 ± 0.008 4	853.2 ± 2.1
0.359 8	995.1 ± 1.6	-174.0 ± 3.4	-0.338 2 ± 0.006 6	942.9 ± 1.9
0.249 8	1001.0 ± 1.4	72.8 ± 3.3	0.081 9 ± 0.003 8	1019.2 ± 1.6
0.159 9	976.6 ± 1.3	439.9 ± 3.2	0.253 4 ± 0.001 8	1064.5 ± 1.5
0.098 97	920.6 ± 2.9	902.5 ± 4.4	0.253 1 ± 0.001 2	1062.6 ± 3.0
0.017 02	598.3 ± 10.0	2937.8 ± 4.1	0.058 76 ± 0.000 08	789.9 ± 10.0
0.009 027	481.9 ± 10.0	3657.1 ± 9.0	0.028 25 ± 0.000 07	655.6 ± 10.0
0.006 618	429.8 ± 3.8	3984.6 ± 12.4	0.019 32 ± 0.000 06	591.8 ± 3.9
0.004 736	377.8 ± 2.1	4315.4 ± 16.4	0.012 67 ± 0.000 05	526.3 ± 2.1
0.003 904	349.9 ± 2.0	4495.0 ± 18.7	0.009 88 ± 0.000 04	490.3 ± 2.1
0.002 870	308.6 ± 2.3	4763.5 ± 22.4	0.006 60 ± 0.000 03	436.2 ± 2.4

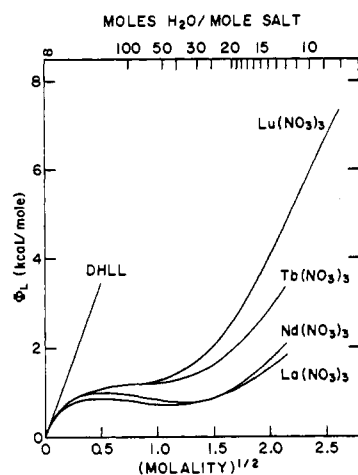


Figure 2. Relative apparent molal enthalpies of La, Nd, Tb, and Lu nitrate solutions at 25 °C.

for dilute rare earth electrolyte solutions, but not at higher concentrations. The dissociation of appreciable amounts of inner sphere nitrate complexes should result in large heat effects. If this is true, the shifting of ϕ_L to lower values for the nitrates implies that heat is absorbed by the dissociation of rare earth nitrate complexes. This is in agreement with values obtained from stability constant studies for dilute solutions (2, 9). The alkaline earth nitrate ϕ_L values are also lower than for the corresponding perchlorate salts (14).

In order to show more details about the crossovers and series trends, series plots of ϕ_L , \bar{L}_2 , and \bar{L}_1 are given in Figures 5–7 at various molalities. The ionic radii were taken from Templeton and Dauben (19). At 0.2 m both the ϕ_L and \bar{L}_2 series exhibit a two-series effect similar to that exhibited by the rare earth perchlorates (16). The minimum in \bar{L}_2 occurs at Pr–Nd and the maximum at Dy (Tb was not run) for the rare earth perchlorates. For the rare earth nitrates this minimum occurs at Sm (Eu was not studied) and the maximum at Ho at 0.2 m. This maximum

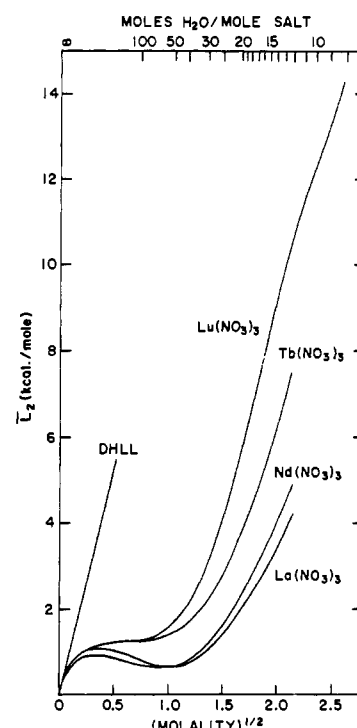


Figure 3. Relative partial molal enthalpies of the solute for La, Nd, Tb, and Lu nitrate solutions at 25 °C.

shifts back to Tb below 0.01–0.02 m for the nitrates, but the minimum stays at Sm to the lowest experimental concentration. However, the experimental error is a significant fraction of the total heat evolved at these very low concentrations, so whether this minimum is actually at Nd or Sm is uncertain. At high concentrations ϕ_L and \bar{L}_2 increase from La to Lu nitrate, but the two-series trend persists for the perchlorates.

It has been suggested that an inner sphere hydration number decrease occurs between Nd and Tb (17) for the rare earth

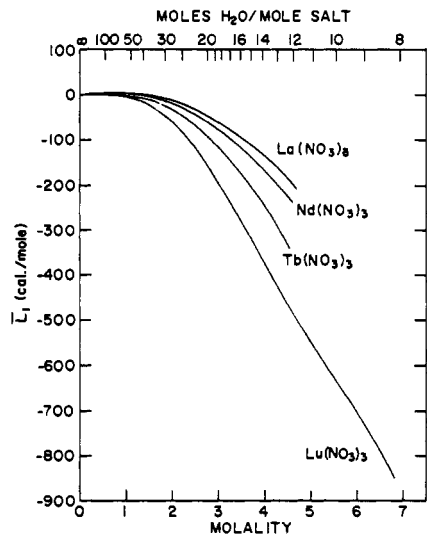


Figure 4. Relative partial molal enthalpies of the solvent for La, Nd, Tb, and Lu nitrate solutions at 25 °C.

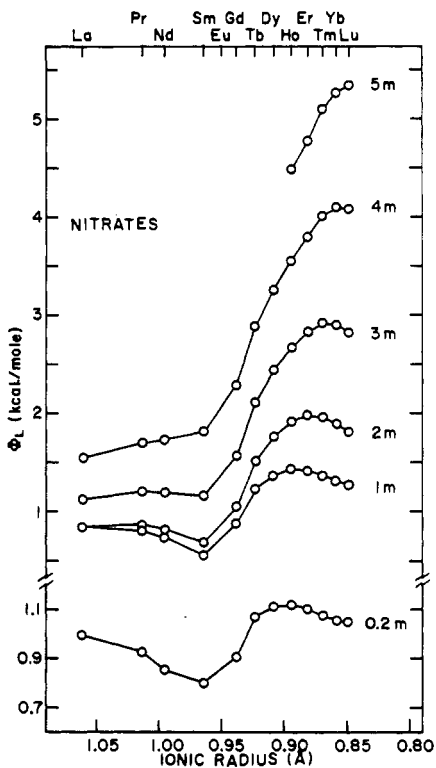


Figure 5. Relative apparent molal enthalpies of rare earth nitrate solutions at constant molalities.

chlorides and perchlorates. In addition, an increase in total hydration occurs, from La to Lu, for these two systems (12). At very low concentrations the rare earth nitrates also show similar behavior. The qualitative features of the rare earth perchlorate heat of dilution data seem to be correlated with these hydration trends (16). This is not the case for the rare earth nitrate solutions above the very dilute range. Considerable amounts of complexed species occur at moderate and high concentrations for the rare earth nitrates. Stability constant measurements for dilute rare earth nitrate solutions (2, 11) indicate that there is a maximum in the amount of rare earth nitrate complex formation at or near Sm. The amount of complex formation increases with concentration, and the electrical conductance data (12) indicate that this maximum in the rare earth series disappears by 0.9 m.

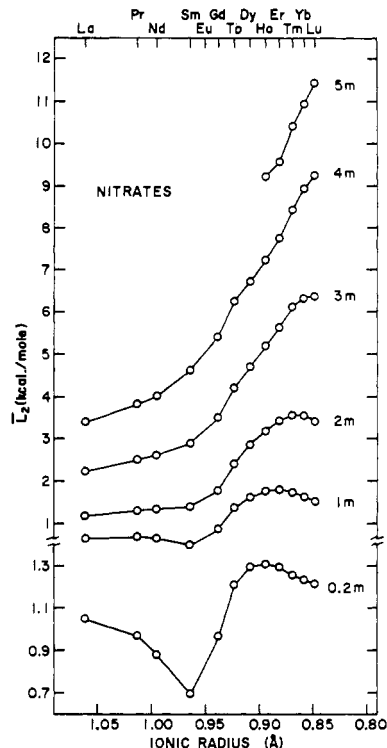


Figure 6. Relative partial molal enthalpies of the solute for rare earth nitrate solutions at constant molalities.

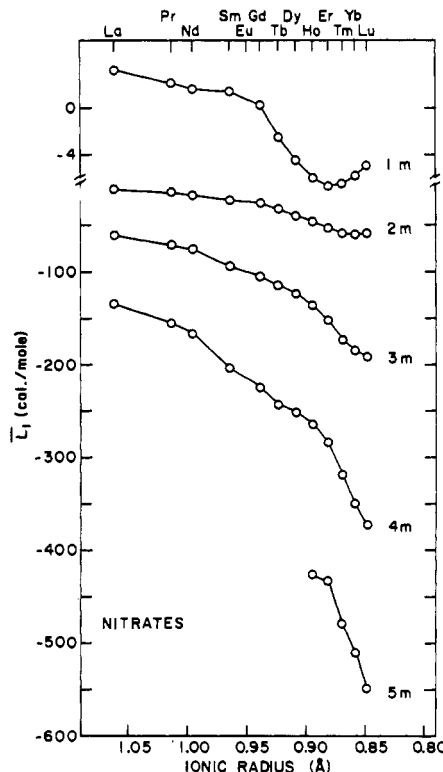


Figure 7. Relative partial molal enthalpies of the solvent for rare earth nitrate solutions at constant molalities.

Above this concentration the amount of complex formation decreases from La to Lu. The heat of dilution data for the rare earth nitrates should correlate with the stability constant trends, especially since the available heats of dissociation for the first nitrate complex are largest for the rare earths with the greatest

amounts of complex formation (9). These heats of dissociation indicate that heat is absorbed for the dissociation process, while the heat of dilution results indicate that heat is still given off for the total dilution process. The dissociation of rare earth nitrate complexes thus reduces the heats of dilution from the amounts that would occur if no complexed species were present. The shift in the minimum for \bar{L}_2 from Pr-Nd (for the perchlorates) to Sm (for the nitrates) and the increase in \bar{L}_2 from La to Lu above 2 m in the nitrates are in agreement with what one would expect from stability constant and heat of dissociation data. In addition, the minimum in \bar{L}_2 at Sm vanishes by 2 m. This is in agreement with the disappearance of the maximum in the amount of complex formation as deduced from electrical conductance data (12).

A number of other anions form complexes with properties similar to the rare earth nitrates. The rare earth sulfate, EDTA, and thiodiacetate complexes (3, 5, 10, 15) exhibit extrema for the stability constants and/or heats of dissociation of these complexes across the rare earth series. These complexes of the rare earth ions might be expected to show similar series trends in the heats of dilution at low concentrations.

Acknowledgment

The rare earth oxides were furnished by the rare earth separation group of the Ames Laboratory. The authors thank A. Habenschuss for suggestions concerning this manuscript and for assistance with the computer programming.

Literature Cited

- (1) Abrahamer, I., Marcus, Y., *Inorg. Chem.*, **6**, 2103 (1967).
- (2) Choppin, G. R., Strazik, W. F., *Inorg. Chem.*, **4**, 1250 (1965).
- (3) Dellien, I., Grenthe, I., Hessler, G., *Acta Chem. Scand.*, **27**, 2431 (1973).
- (4) Derer, J. L., Ph.D. dissertation, Iowa State University, Ames, Iowa, 1974.
- (5) Farrow, M. M., Purdie, N., *J. Solution Chem.*, **2**, 503 (1973).
- (6) Garnsey, R., Ebdon, D. W., *J. Am. Chem. Soc.*, **91**, 50 (1969).
- (7) Gucker, F. T., Pickard, H. B., Planck, R. W., *J. Am. Chem. Soc.*, **61**, 459 (1939).
- (8) Mohs, M. A., Ph.D. dissertation, Iowa State University, Ames, Iowa, 1970.
- (9) Moulin, N., Hussonnois, M., Brillat, L., Guillaumont, R., *J. Inorg. Nucl. Chem.*, **37**, 2521 (1975).
- (10) Ots, H., *Acta Chem. Scand.*, **27**, 2344 (1973).
- (11) Peppard, D. F., Mason, G. W., Hucher, I., *J. Inorg. Nucl. Chem.*, **24**, 881 (1962).
- (12) Rard, J. A., Spedding, F. H., *J. Phys. Chem.*, **79**, 257 (1975).
- (13) Rard, J. A., Spedding, F. H., Shiers, L. E., Heiser, D. J., unpublished data.
- (14) Rossini, F. D., Wagman, D. D., Evans, W. H., Levine, S., Jaffe, I., *Natl. Bur. Stand. (U.S.) Circ.*, No. 500 (1952).
- (15) Spedding, F. H., Jaffe, S., *J. Am. Chem. Soc.*, **78**, 882 (1954).
- (16) Spedding, F. H., Mohs, M. M., Derer, J. L., Habenschuss, A., *J. Chem. Eng. Data*, in press.
- (17) Spedding, F. H., Pikal, M. J., Ayers, B. O., *J. Phys. Chem.*, **70**, 2440 (1966).
- (18) Spedding, F. H., Shiers, L. E., Brown, M. A., Baker, J. L., Gutierrez, L., McDowell, L. S., Habenschuss, A., *J. Phys. Chem.*, **79**, 1087 (1975).
- (19) Templeton, D. H., Dauben, C. H., *J. Am. Chem. Soc.*, **76**, 5237 (1954).

Received for review March 9, 1976. Accepted June 8, 1976. This work was performed for the U.S. Energy Research and Development Administration under Contract No. W-7405-eng-82. This report is based, in part, on the Ph.D. dissertations of M. A. Mohs, 1970, and J. L. Derer, 1974, at Iowa State University, Ames, Iowa.

Solubilities of Heavy Hydrocarbons in Compressed Methane and Nitrogen

Saul G. D'Avila,[†] Bal K. Kaul, and John M. Prausnitz*

Chemical Engineering Department, University of California, Berkeley, California 94720

Vapor-phase solubilities of *n*-decane, 2,2,5-trimethylhexane, *tert*-butylbenzene, and *n*-dodecane were measured in compressed methane and in compressed nitrogen. Measurements were taken in the range 30–100 atm and 25–125 °C. From these measurements, second virial cross coefficients B_{12} were calculated with a maximum uncertainty of $\pm 10 \text{ cm}^3 \text{ mol}^{-1}$.

Interactions between molecules of common nonpolar gases (e.g., N_2 and methane) are now reasonably well understood but little is known about the interactions of such gases with large hydrocarbons. An understanding of these interactions is becoming of increasing importance in technology as development of new processes concerned with gasification of coal and heavy petroleum is stimulated by changes in the world's energy supply.

In several recent publications from this laboratory, experimental solubility data were reported for a number of gaseous solutes in heavy hydrocarbon solvents (3, 4, 11). These data, in the form of Henry's constants, supply fundamental information

on the behavior of a small molecule (e.g., methane) when it is completely surrounded by large hydrocarbon molecules in the liquid phase. In the work presented here, we report some experimental solubility data on the other end of the composition spectrum: the behavior of a large hydrocarbon molecule completely surrounded by small molecules in the gas phase. These data, in the form of second virial cross coefficients, give fundamental information on the potential energy function for dissimilar molecules. More important for technological application, these data are useful for estimating solvent losses in high-pressure absorbers and for estimating dew points in gas mixtures containing small amounts of heavy hydrocarbon components such as tars.

Experimental Section

The experimental technique used for solubility measurements is essentially the same as that used by Rigby (10) and Benson (2). Figure 1 presents a schematic diagram of the apparatus. Hydrocarbon liquid is placed in each of two equilibrium cells, arranged in series. High-pressure gas, entering through spargers at the bottom of each cell, slowly bubbles through the liquid; the gas leaving the second equilibrium cell is saturated with the heavy component. Two cells in series are used to assure saturation. The high-pressure, gas-phase mixture leaving the second

* Now at Departamento de Engenharia Química, Universidade de Campinas, 13100 Campinas, Brazil.